Hindawi
International Journal of Aerospace Engineering
Volume 2023, Article ID 7644738, 15 pages
https://doi.org/10.1155/2023/7644738

Research Article

Simplified Mixing Rules for Calculating Transport Coefficients of High-Temperature Air

Zhe Wang, Yufeng Han, and Wei Cao

Department of Mechanics, Tianjin University, Tianjin 30072, China

Correspondence should be addressed to Wei Cao; 2016201044@tju.edu.cn

Received 8 September 2022; Revised 9 January 2023; Accepted 13 January 2023; Published 27 January 2023

Academic Editor: Adel Ghenaiet

Copyright © 2023 Zhe Wang et al. This is an open access article distributed under the Creative Commons Attribution License, which permits unrestricted use, distribution, and reproduction in any medium, provided the original work is properly cited.

The transport process of high-temperature air is vital in aerospace fields and has attracted increased attention in recent years. In this paper, an adequate study of factors affecting transport coefficients for high-temperature air is conducted. The results of a different-species model at different pressures and temperatures show that the 9-species air model is applicable to calculate the viscosity and translational thermal conductivity coefficients before significant ionization occurs. Based on the Chapman-Enskog method, simplified mixing rules for calculating viscosity and translational thermal conductivity coefficients of high-temperature air are developed by omitting unimportant matrix elements and assuming the reduced collision integral ratio to a reasonable constant value. The diagonal elements' magnitude of the transport matrix indicates that collision related to the electrons has a little impact on viscosity but has a great influence on translational thermal conductivity. New simplified mixing rules can accurately calculate the viscosity and translational thermal conductivity coefficients of high-temperature air when dissociation or weak ionization occurs. The improved mixing rules are obviously more accurate than the Wilke mixing rule.

1. Introduction

In hypersonic flight, the strong aerodynamic heating and viscous dissipation can cause an extremely high temperature (even exceeding 10,000 K) of the air mixture surrounding the vehicle, such as in the shock wave, at the stagnation point, and in the boundary layer, which may lead to vibration, dissociation, chemical reaction, and even ionization of the gas molecules. The thermodynamic and transport properties of high-temperature air are vastly changed and deviate far from a perfect gas [1]. Variation of the transport properties significantly affects the flow properties and aerothermodynamics, which is especially important for the development of hypersonic vehicles [2]. Therefore, accurate estimates of the viscosity and thermal conductivity coefficients to represent correctly momentum and energy transport are a crucial prerequisite for hypersonic flow simulation. In general, the coefficient of viscosity is used to describe the shear forces caused by velocity gradients. The coefficient of thermal conductivity is heat conduction caused by temperature gradients [3–5].

Physically, the transport phenomenon is essentially caused by collisions and free movement of molecules, atoms, ions, and electrons in gas mixtures. The transport process can be accurately described by the Boltzmann equation, which is a seven-dimensional integral-differential equation. However, it is extremely difficult to solve this equation directly. The transport coefficients of local-equilibrium gas can be calculated using the Chapman-Enskog (CE) approximation with a finite Sonine polynomial expansion of the Boltzmann equation [6, 7]. The proportions of each component and collision integrals between species in the CE approximation are two essential aspects for calculating the transport coefficients. The proportion of each component can be obtained by solving the equations of chemical reaction, while the collision integrals between species can be calculated by integrating the interaction potential between species. In hypersonic flight, the air over a vehicle is often in chemical nonequilibrium. The transport properties should be simulated considering nonequilibrium effects. However, up to now, there is no consensus on the modified decoupling model of the CE method for

Table 1: Summary of collision integrals and transport coefficients proposed by different authors.

	Reference	Data type	Temperature and pressure range
Collision integrals	Yun and Mason [13]	Data table	1000 K-15,000 K
	Gupta et al. [15]	Fitting expression	1000 K-30,000 K
	Capitelli et al. [17]	Fitting expression	50 K-100,000 K
	Wright et al. [20]	Fitting expression	300 K-15,000 K
Transport coefficients	Hansen [31]	Data table	500 K-15,000 K, 10^{-4} atm-100 atm
	Yos [14]	Data table	1000 K-30,000 K, 1 atm-30 atm
	Srinivasan [32]	Fitting expression	500 K-16,500 K, 10^{-5} atm-10 atm
	Gupta et al. [15]	Fitting expression (single species)	1000 K-30,000 K
	Murphy [16]	Data graph	100 K-30,000 K 1 atm
	Capitelli et al. [18]	Fitting expression	50 K-100,000 K, 0.01 atm-100 atm
The mixing rules[a]	Buddenberg and Wilke [21], Yos [14], Armaly and Sutton [27], Copeland [24]		

[a]The mixing rules of calculating transport coefficients require information about the transport coefficients of a single species.

the nonequilibrium transport properties [8, 9]. As a compromise, most of the present computational fluid dynamic simulations are based on transport coefficients under equilibrium condition [10–12].

It is difficult to measure transport coefficients of high-temperature air in the experiment, so most of the current research focus on theoretical calculation by using the CE method. With the development of quantum chemistry, the collision integrals between two species are studied in depth. Thus, transport coefficients are often updated. Yun and Mason [13] published the collision integrals for atom-atom, atom-molecule, and molecule-molecule interactions of high-temperature air in the temperature range of 1000 K to 15,000 K. Yos [14] calculated the transport coefficients of hydrogen, oxygen, nitrogen, and air in the temperature range of 1000 K-30,000 K at 1-30 atm. Later, Gupta et al. [15] provided not only the fitting expression of collision integrals between species but also that of transport coefficients for the air species in the temperature range of 1000 K-30,000 K. These fitting expressions are largely based on the data tables from Yun and Mason [13] and Yos [14] and are still widely used so far. The above studies focus on the transport coefficients when the temperature is higher than 1000 K. In addition to these studies, subsequent research considers the temperature below 1000 K. Murphy [16] considered that air is composed of 78.09% nitrogen, 20.94% oxygen, 0.93% argon, and 0.033% carbon dioxide in the temperature range of 300 K-30,000 K. It is found that carbon dioxide can cause a difference in viscosity by about 15%. Capitelli et al. [17, 18] calculated and fitted the collision integrals of air species by comparing existing transport cross-section data in the temperature range of 50 K-100,000 K. He pointed out that Gupta et al.'s [15] fitting data are notably outdated. The transport coefficients of Capitelli are in good agreement with those of Yun and Mason [13] but differ from those of Yos [14] with 30-35%. Subsequently, D'Angola et al. [19] fitted the computational results of thermodynamic and transport coefficients of equilibrium air with 19 species into algebraic expressions in the temperature range of 50 K-60,000 K, but the pressure range is limited to 0.01-100 atm. Wright et al. [20] reviewed the development of collision integrals for weakly ionized air species in the temperature range of 300 K-15,000 K and also mentioned that Gupta et al.'s [15] fitting data have largely become obsolete. A major difference when employing the CE method is the wide variety of collision integrals, which oftentimes led to differences in the transport coefficients.

The accuracy required for transport coefficients must be balanced with the computational costs during the practice. Thus, by simplifying the CE approximation, the need for mixing rules of calculating transport coefficients is an interesting subject. Up to now, the Wilke mixing rule [21] is one of the most widely used approximate methods [22, 23]. It ignored the nondiagonal elements of the transport matrix and then assumed that all the reduced collision integral ratios in the diagonal elements are one. Yos [14] also derived a simplified rule applicable to weak ionization and nonionization conditions by ignoring the off-diagonal elements of the transport matrix. But this rule requires large amounts of collision integrals between heterogeneous species so that it is inconvenient to use. Recently, Copeland [24] retained the off-diagonal elements of the transport matrix and proposed a simplified rule by approximating the reduced collision integral ratio to 10/9, which can be used to calculate the transport coefficients of polar and nonpolar particle mixtures. This rule is proven to be more accurate than the Wilke mixing rule [21], but its simplicity is lost. In addition, several other mixing rules [25–27] are developed based on the CE method, and these mixing rules are evaluated in terms of efficiency and accuracy [28–30]. These approximate methods usually cannot address the dual requirements of simple formula and physical accuracy.

Collision integrals and typical transport coefficients proposed by different authors are summarized in Table 1. Among all these methods, the CE method is the most accurate for calculating the transport coefficients. However, it needs to collect a large number of collision integrals and numerically solve the matrix equations, which will lead to lower computational efficiency. The Wilke mixing rule is simple enough but loses accuracy. At present, other existing approximate methods are too complex to use. On this basis, the purpose of this paper is to propose simplified mixing

rules to accurately estimate the transport coefficients for high-temperature air. Firstly, each component of air that mainly affects the transport process is studied. Then, the influence of the matrix element and the reduced collision integral ratio of the transport matrix is analyzed. Finally, simplified mixing rules are developed for accurately estimating the viscosity and translational thermal conductivity coefficients. And the validation of mixing rules is being conducted at different pressures.

2. Numerical Method and Code Validation

2.1. The CE Method. The CE method for viscosity and translational thermal conductivity coefficients includes three processes.

2.1.1. Calculation of the Proportion for Each Component. At room temperature, the air is a mixture of nitrogen and oxygen. With the increase of temperature, the air will undergo dissociation and ionization reactions, so the proportion of each component of high-temperature air will change accordingly. The mole fraction of each component can be obtained by solving the chemical reaction equations.

2.1.2. Calculation of the Collision Integrals between Species. The collision integrals between two species are tabulated for many intermolecular potentials and are available in the literature. Considering a N-species air mixture, it is necessary to obtain collision integrals of $N^*\ (N+1)/2$. The interaction between species mainly includes the following four categories: the interactions between neutral species, the interactions between electrons and neutral species, the interactions between ions and neutral species, and the interactions between charged species.

2.1.3. Calculation of the Viscosity and Translational Thermal Conductivity Coefficients

(a) The viscosity coefficients can be expressed as

$$\mu = \sum_{j=1}^{n} x_j \overline{b_{j0}}(1), \tag{1}$$

where x_j is the mole fraction of species j and n is the number of species. $\overline{b_{j0}}(1)$ are Sonine expansion coefficients. Parameter 1 in the brackets represents the first-order expansion. $\overline{b_{j0}}(1)$ are obtained by solving the linear system $\sum_{j=1}^{n} \mathbf{H_{ij}} \overline{b_{j0}}(1) = x_i$. The matrix elements of $\mathbf{H}$ are

$$\mathbf{H_{ii}} = \frac{x_i^2}{\mu_i} + \sum_{\substack{j=1 \\ j\neq i}}^{n} \frac{2x_i x_j}{\mu_{ij}} \frac{M_i M_j}{\left(M_i + M_j\right)^2} \left[\frac{5}{3A_{ij}^*} + \frac{M_j}{M_i}\right], \tag{2}$$

$$\mathbf{H_{ij}} = -\frac{2x_i x_j}{\mu_{ij}} \frac{M_i M_j}{\left(M_i + M_j\right)^2} \left[\frac{5}{3A_{ij}^*} - 1\right], \tag{3}$$

where $A_{ij}^* = \Omega_{ij}^{(2,2)*}/\Omega_{ij}^{(1,1)*}$ is a ratio of reduced collision integral and $A_{ij}^* = A_{ji}^*$. $\Omega_{ij}^{(l,s)*}$ is the reduced collision integrals between species i and species j. $l = 1$ or 2 represents the diffusion collision integrals of mass transport and the viscous collision integrals of momentum transport, respectively. s represents the collision integrals of the same type in different orders. M_i is the molecular weight of the species i. μ_i is the viscosity of pure species i, which is

$$\mu_i = \frac{\sqrt{2}}{52979} \frac{\sqrt{M_i T}}{\Omega_{ii}^{(2,2)*}}, \tag{4a}$$

and μ_{ij} is the collision viscosity between species i and species j, which is

$$\mu_{ij} = \frac{\sqrt{2}}{52979} \frac{\sqrt{2M_i M_j T/\left(M_i + M_j\right)}}{\Omega_{ij}^{(2,2)*}}. \tag{4b}$$

(b) The translational thermal conductivity coefficients can be expressed as

$$k_{tr} = \sum_{j=1}^{n} x_j \overline{a_{j1}}(2). \tag{5}$$

The Sonine expansion coefficients $\overline{a_{j1}}(2)$ are obtained by solving the linear system $\sum_{j=1}^{n} \mathbf{L_{ij}} \overline{a_{j1}}(2) = x_i$. The matrix elements of $\mathbf{L}$ are

$$\mathbf{L_{ii}} = \frac{x_i^2}{\lambda_i} + \sum_{\substack{j=1 \\ j\neq i}}^{n} \frac{x_i x_j \left((15/2)M_i^2 + (25/4)M_j^2 - 3M_j^2 B_{ij}^* + 4M_i M_j A_{ij}^*\right)}{2\left[\left(M_i + M_j\right)^2 A_{ij}^* \lambda_{ij}\right]}, \tag{6}$$

$$\mathbf{L_{ij}} = -\frac{x_i x_j M_i M_j \left(55/4 - 3B_{ij}^* - 4A_{ij}^*\right)}{2\left[\left(M_i + M_j\right)^2 \lambda_{ij} A_{ij}^*\right]}, \tag{7}$$

where $B_{ij}^* = (5\Omega_{ij}^{(1,2)*} - 4\Omega_{ij}^{(1,3)*})/\Omega_{ij}^{(1,1)*}$ is another ratio of reduced collision integral and $B_{ij}^* = B_{ji}^*$. λ_i is the translational thermal conductivity of species i, which is

$$\lambda_i = \frac{15}{4} \frac{R}{M_i} \mu_i, \tag{8a}$$

and λ_{ij} is the collision translational thermal conductivity between species i and species j, which is

$$\lambda_{ij} = \frac{15}{4} \frac{R}{2M_i M_j/\left(M_i + M_j\right)} \mu_{ij}, \tag{8b}$$

where R is the universal gas constant.

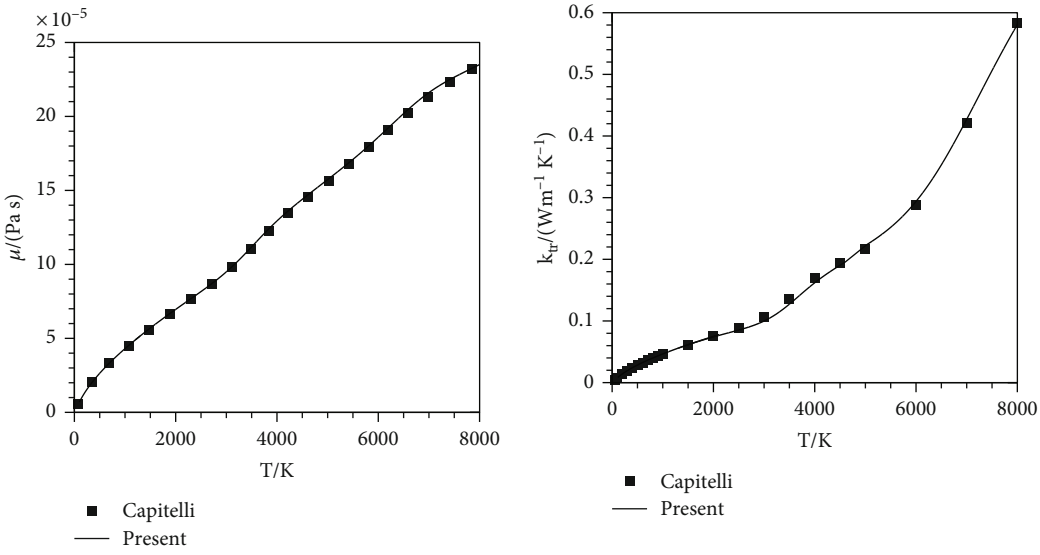

Figure 1: Comparison of the present results with Capitelli et al. [18]. (a) Viscosity; (b) translational thermal conductivity.

2.2. Code Validation for the CE Method. The comparisons of viscosity and translational thermal conductivity coefficients between the present results and those obtained by Capitelli et al. [18] in the temperature range of 50 K-8000 K at 1 atm are presented in Figure 1. Capitelli used a 19-species model to calculate the transport coefficients. Because the temperature is lower than 8000 K, the main reaction is dissociation and ionization of the air. For simplicity, the 9-species model is enough to cover the overall involved reaction, for which it is adopted in the present validation. The collision integrals are calculated by the fitting expression from Capitelli et al. [17] and Wright et al. [20]. One can see that the present calculation results are in good agreement with the results of Capitelli, indicating that the code for the CE method used in this study is reliable. In addition, the results confirm that the 9-species model is sufficient in the temperature range of 50 K-8000 K at 1 atm.

It should be mentioned that the total thermal conductivity of gas consists of translational, internal, and reactive thermal conductivity when the components of a gas mixture react with one another. Together, the translational and internal thermal conductivities are also referred to as the frozen thermal conductivity, including the contribution of translational and internal degrees of freedom. The reactive thermal conductivity is due to the energy released or absorbed from chemical reactions. Usually, the simplified expression of Hirschfelder [6] can be used for the internal thermal conductivity. The reactive thermal conductivity can be calculated with the formula of Butler and Brokaw [33]. Traditionally, the mixing rules are used to compute translational thermal conductivity. The present study focuses only on the translational part because it is a fundamental thermal conductivity mechanism.

3. Results and Discussion

Firstly, the effect of the species model at different pressures is studied in Section 3.1. Then, the influence of matrix elements and the reduced collision integral ratio in equations (2) and (3) and equations (6) and (7) is analyzed. Accordingly, simplified mixing rules are developed by omitting unimportant matrix elements and making some reasonable assumptions to the reduced collision integral ratio in Section 3.2. Finally, validation of cases using the new simplified mixing rules is presented in Section 3.3.

The atmospheric pressure decreases with the increase of altitude, so the pressure range considered in this paper is below 1 atm. In general, partial ionization of air occurs when the temperature reaches 8000 K. This study focuses on the air without significant ionization, so the highest temperature is limited to 8000 K.

3.1. Effect of Species Model on the Viscosity and Translational Thermal Conductivity Coefficients at Different Pressures. Depending on the degree of chemical reaction, the mixture may contain different species. In general, 2-species (N_2, O_2), 5-species (N_2, O_2, N, O, NO), 7-species ($N_2, O_2, N, O, NO, NO^+, e^-$), 9-species ($N_2, O_2, N, O, NO, NO^+, e^-, N^+, O^+$), and 11-species ($N_2, O_2, N, O, NO, NO^+, e^-, N^+, O^+, N_2^+, O_2^+$) mode can be used in the simulation. Because the calculation of transport coefficients requires a large number of collision integrals, an appropriate species model should be chosen at first.

Figure 2 shows the results of viscosity coefficients obtained by using a different-species model at $P = 0.001$ atm, 0.01 atm, 0.1 atm, and 1 atm. Figure 2(a) presents a comparison of viscosity coefficients using the different-species model at 0.001 atm. It can be seen that the viscosity coefficients calculated by the 2-species model are clearly lower than other models when $T > 2000$ K. The discrepancy between the 5-species model and the 7-species model is very slight. This is because the molar fraction of NO^+ and e^- is very low. The viscosity coefficients of the 5-species model or the 7-species model will keep increasing with the increase of temperature, while the results of the 9-species model

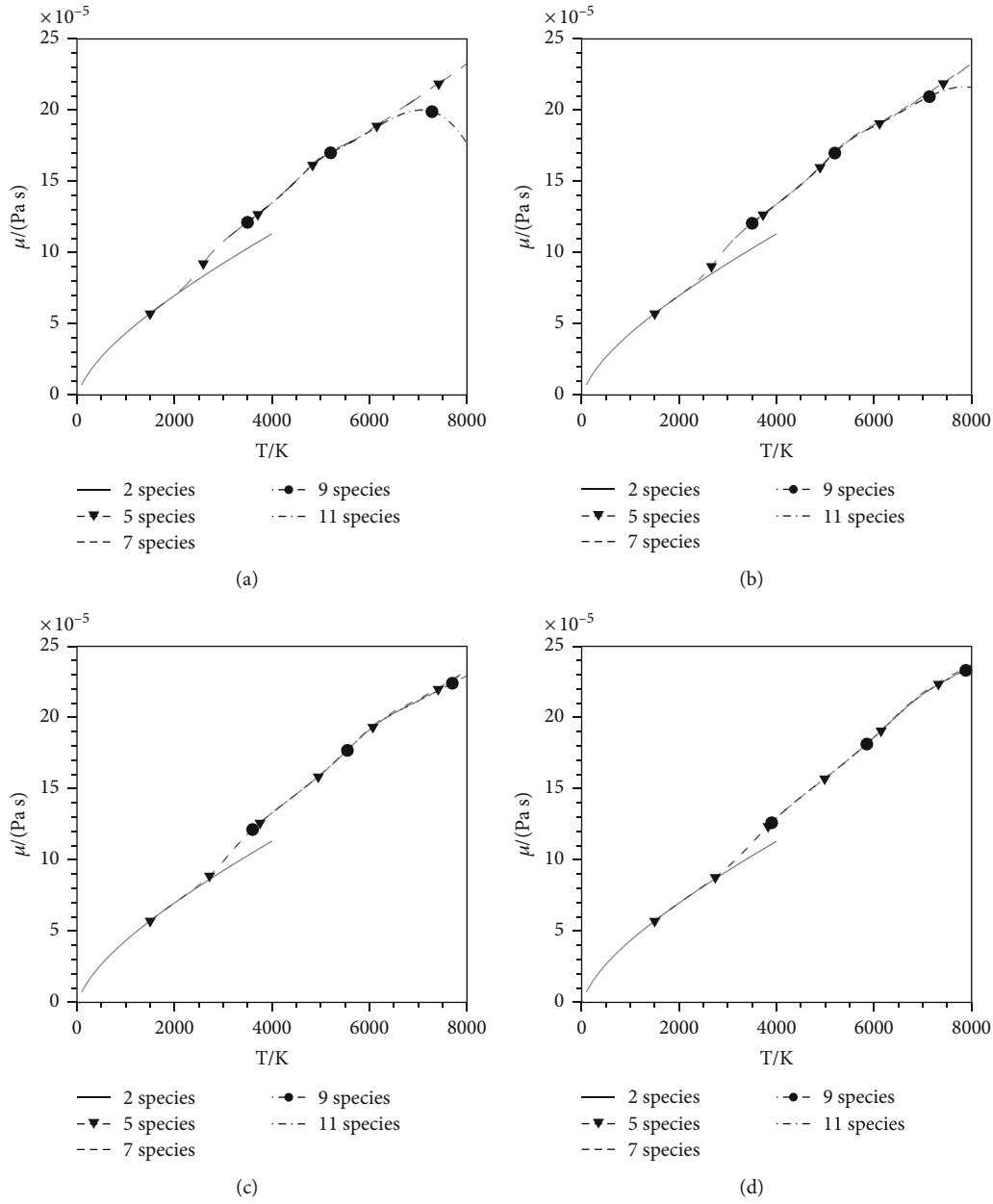

Figure 2: Viscosity coefficients at different pressure conditions. (a) 0.001 atm, (b) 0.01 atm, (c) 0.1 atm, and (d) 1 atm.

decrease when $T > 7000$ K. This is because N^+, O^+, and e^- are gradually produced; their collision integrals are larger than those between neutral species, resulting in the decrease of viscosity. The results of the 9-species model and the 11-species model are almost consistent, owing to the fact that the amount of N_2^+ and O_2^+ is very small. The trends between these species model are similar for $P = 0.01$ atm, 0.1 atm, and 1 atm, as shown in Figures 2(b)–2(d), respectively. These results indicate that the 9-species model is sufficient to calculate the viscosity coefficients.

Figure 3 shows the results of translational thermal conductivity coefficients obtained by using the different-species model at $P = 0.001$ atm, 0.01 atm, 0.1 atm, and 1 atm. It can be seen that the effect of species and pressure on translational thermal conductivity coefficients is consistent with that of viscosity coefficients. These results indicate that the 9-species model is also capable of calculating the translational thermal conductivity coefficients. In addition, by comparing Figures 2(a) and 3(a), one can see that the viscosity coefficients between the 7-species model and the 9-species model have a difference when $T > 6000$ K, while the translational thermal conductivity coefficients between the 7-species model and the 9-species model are different when $T > 5000$ K. Weak ionization occurs at about 5000 K, causing little ions and electrons in the air mixture. This reveals that in the initial stage of ionization, a small number of charged species have a greater impact on the translational thermal conductivity but have a little impact on the viscosity.

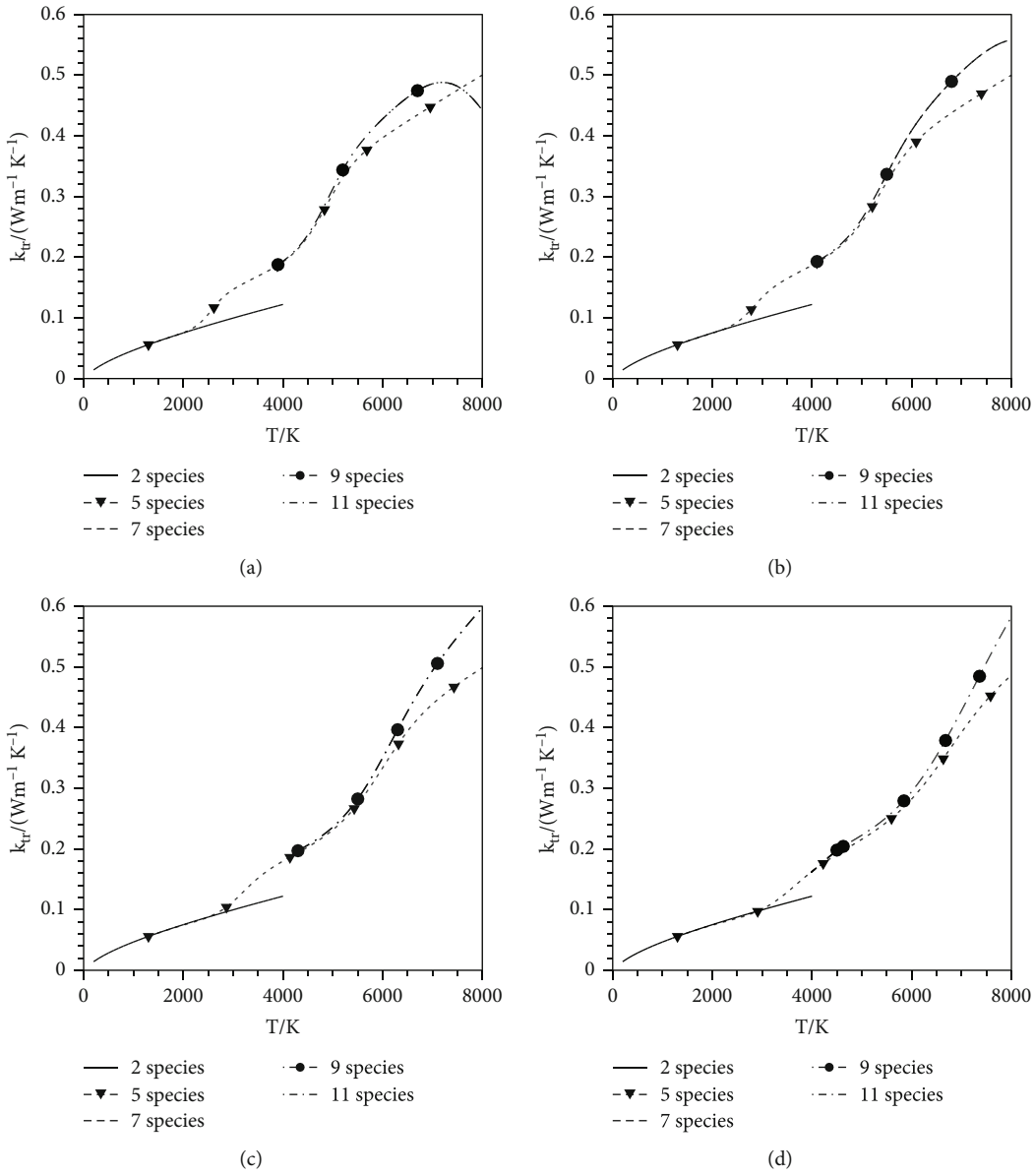

Figure 3: Translational thermal conductivity coefficients at different pressure conditions. (a) 0.001 atm, (b) 0.01 atm, (c) 0.1 atm, and (d) 1 atm.

3.2. Simplified Mixing Rules Based on the Chapman-Enskog Method. The detailed deriving process can be divided into four steps.

3.2.1. Evaluating Off-Diagonal Elements' Effect. Previous research has shown that **H** and **L** are a diagonally dominant matrix [15, 26, 28]. The deviation brought by off-diagonal elements of the transport matrix is analyzed. Figure 4 presents the viscosity and translational thermal conductivity coefficients of the CE method while retaining and omitting the off-diagonal elements at 0.001 atm. Figure 4(a) shows the results of the viscosity; it can be seen that the viscosity coefficients decrease when omitting the off-diagonal elements. Similarly, the translational thermal conductivity coefficients (shown in Figure 4(b)) will decrease when the off-diagonal elements are omitted. The differences of viscosity coefficients while retaining and omitting the off-diagonal elements of the matrix are about 5.8%, while for the translational thermal conductivity coefficients, there is a deviation of 11.3%. Because the off-diagonal member of the matrix $\mathbf{H}_{ij}$ is much smaller than the diagonal member $\mathbf{H}_{ii}$, it is ignored in the present study.

3.2.2. Evaluating Diagonal Elements' Magnitude. Omitting the off-diagonal elements in equations (1) and (5), we get

$$\mu = \sum_{i=1}^{n} \frac{x_i^2}{\mathbf{H_{ii}}}, \tag{9}$$

$$k_{tr} = \sum_{i=1}^{n} \frac{x_i^2}{\mathbf{L_{ii}}}. \tag{10}$$

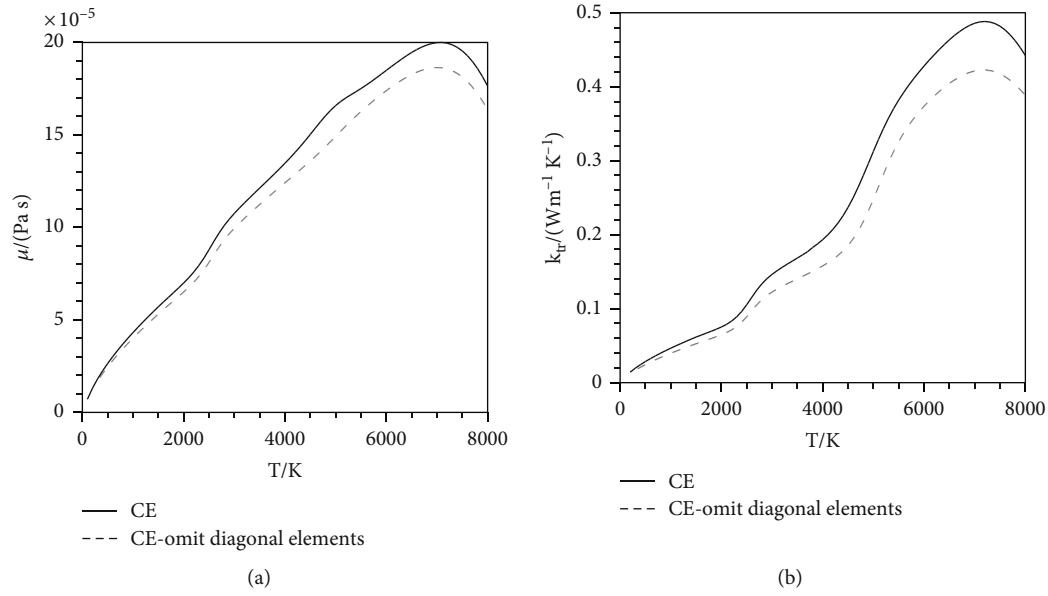

Figure 4: Effect of off-diagonal elements on viscosity and translational thermal conductivity. (a) Viscosity; (b) translational thermal conductivity.

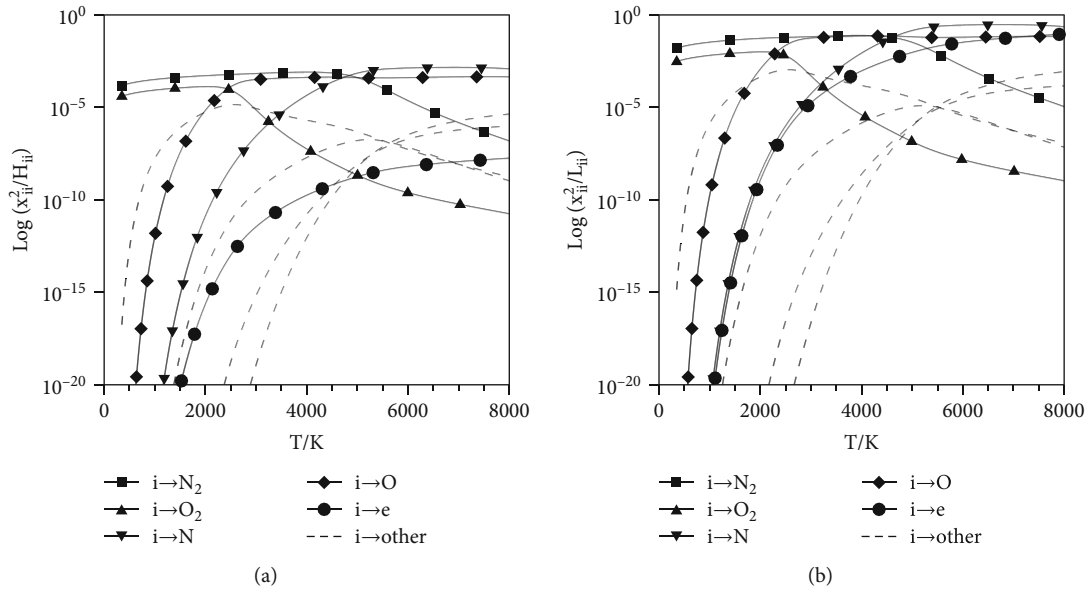

Figure 5: The size of each term of viscosity and translational thermal conductivity coefficients. (a) Viscosity; (b) translational thermal conductivity.

The magnitude of the diagonal elements is evaluated. Figure 5 shows the size of each term in equations (9) and (10) at 0.001 atm. Label $i \longrightarrow$ other represents the species NO, NO^+, N^+, O^+. Figure 5(a) presents the size of $x_i^2/\mathbf{H_{ii}}$. In the temperature range of 50 K-2000 K, the magnitude of $x_{O_2}^2/H_{O_2O_2}$ and $x_{N_2}^2/H_{N_2N_2}$ is largest. This indicates that the first effect on viscosity is the collision related to nitrogen and oxygen molecules. When $T > 2500$ K, the magnitude of $x_{O_2}^2/H_{O_2O_2}$ is lower than that of x_O^2/H_{OO}. When $T > 4500$ K , the magnitude of $x_{N_2}^2/H_{N_2N_2}$ is lower than that of x_N^2/H_{NN} . The results demonstrate that the collision related to nitrogen and oxygen atoms begins to have a major impact when dissociation occurs. The trend of translational thermal conductivity is similar for molecules and atoms (shown in Figure 5(b)). When $T > 5000$ K, weak ionization occurs; it is seen from Figure 5(a) that the magnitude of x_e^2/H_{ee} is lower than those of x_O^2/H_{OO} and x_N^2/H_{NN}, which indicates that collision related to the electrons has a little impact on viscosity. However, as shown in Figure 5(b), the magnitude of x_e^2/H_{ee} is the same with those of x_O^2/H_{OO} and x_N^2/H_{NN}, which indicates that collision related to the electrons has a great influence on translational thermal conductivity. Other

terms' magnitude of equations (9) and (10) is lower, indicating that the influence of the collision related to ions is not dominated.

3.2.3. Simplification for the Reduced Collision Integral Ratios A_{ij}^* and B_{ij}^*. Substituting equations (2) and (6) into equations (9) and (10), respectively, and rearranging, we have

$$\mu = \sum_{i=1}^{n} \frac{\mu_i}{1 + \sum_{\substack{j=1 \\ j\neq i}}^{n} F_{ij}^*\left(x_j/x_i\right)\sqrt{2M_j}\left(\left[\left(5/3A_{ij}^*\right)M_i + M_j\right]/\left(M_i + M_j\right)^{3/2}\right)}, \tag{11}$$

$$k_{tr} = \sum_{i=1}^{n} \frac{\lambda_i}{1 + \sum_{\substack{j=1 \\ j\neq i}}^{n} F_{ij}^*\left(x_j/x_i\right)\sqrt{2M_j/\left(M_i + M_j\right)}} \times \frac{1}{\left[(15/2)M_i^2 + (25/4)M_j^2 - 3M_j^2B_{ij}^* + 4M_iM_jA_{ij}^*\right]/2\left[\left(M_i + M_j\right)^2A_{ij}^*\right]}, \tag{12}$$

where $F_{ij}^* = \Omega_{ij}^{(2,2)*}/\Omega_{ii}^{(2,2)*}$ represents a reduced ratio of the viscous collision integral of heterogeneous species to homogeneous species, unlike the reduced collision integral ratio A_{ij}^* and B_{ij}^*, while for the reduced collision integral ratio F_{ij}^*, $F_{ij}^* \neq F_{ji}^*$.

The reduced collision integral ratios A_{ij}^* and B_{ij}^* in equations (11) and (12) are single-valued functions of temperature. Figure 6 presents the A_{ij}^* of neutral species. It can be seen that the A_{ij}^* of neutral species increases monotonically in the range of 1.1 to 1.25 with the increase of temperature. In order to simplify equation (11), we take three different assumptions of A_{ij}^* for all interactions. Figure 7 shows the relative deviation of viscosity between equation (11) and the CE method at 0.001 atm. It can be seen that when A_{ij}^* is chosen as 6/5 (between 1.1 and 1.25), the results of equation (11) will obviously deviate from the CE method and so does the chosen of 6/3 for A_{ij}^*. When A_{ij}^* is assumed as 5/3, the results of equation (11) are in the best agreement with those of the CE method. This assumption is out of the range at 1.1 to 1.25 as shown in Figure 6, because the initial assumption of omitting the off-diagonal elements will lead to a reduction of viscosity coefficients. A relatively larger A_{ij}^* can make up for this reduction. Therefore, simplification of 5/3 for A_{ij}^* is reasonable. Thus, we obtain a simple form for viscosity:

$$\mu = \sum_{i=1}^{n} \frac{\mu_i}{1 + \sum_{\substack{j=1 \\ j\neq i}}^{n} F_{ij}^*\left(x_j/x_i\right)\sqrt{2M_j/\left(M_i + M_j\right)}}. \tag{13}$$

It is worth mentioning that when $T > 7000$ K, significant ionization occurs and relative deviation will increase obviously.

Figure 8 shows the reduced collision integral ratio B_{ij}^* of neutral species in equation (12). It can be seen that the $B_{N_2O_2}^*$ decreases from 1.2 to 0.5 and the B_{NO}^* increases from 1.8 to 2.5 with increasing temperature. The B_{ij}^* for interactions between molecules and atoms are around 1.1. Figure 9 shows the B_{ij}^* for interactions between electrons and other particles. It can be seen that the $B_{eN^+}^*$ and $B_{eO^+}^*$ are about 1.1. In order to simplify equation (12), we take three different assumptions of B_{ij}^* for all interactions. Figure 10 shows the relative deviation of translational thermal conductivity coefficients between equation (5) and the CE method at 0.001 atm. It can be seen that the relative deviation is less than 10% at different assumption of B_{ij}^*. It implies that the effect of B_{ij}^* on the translational thermal conductivity is slight. When B_{ij}^* is assumed as 5/4, the results of equation (5) are in the best

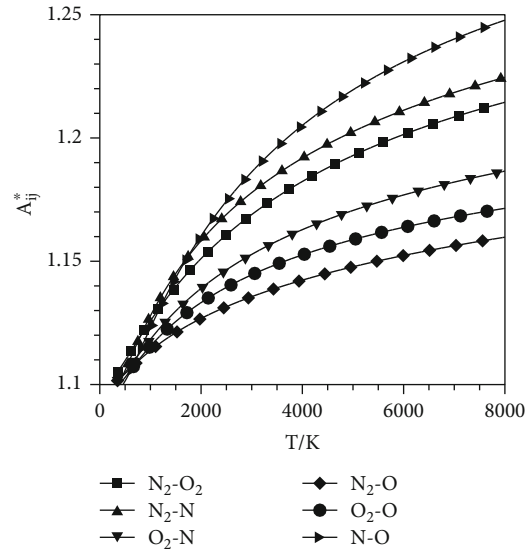

Figure 6: A_{ij}^* between neutral species.

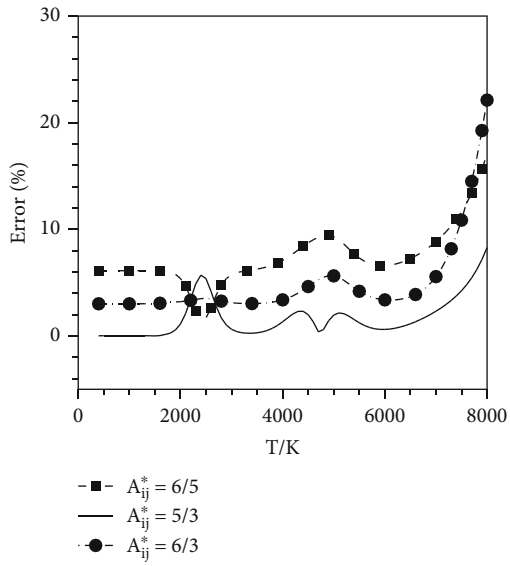

Figure 7: Relative deviation of viscosity between equation (11) at three assumptions of A_{ij}^* and the CE method at 0.001 atm.

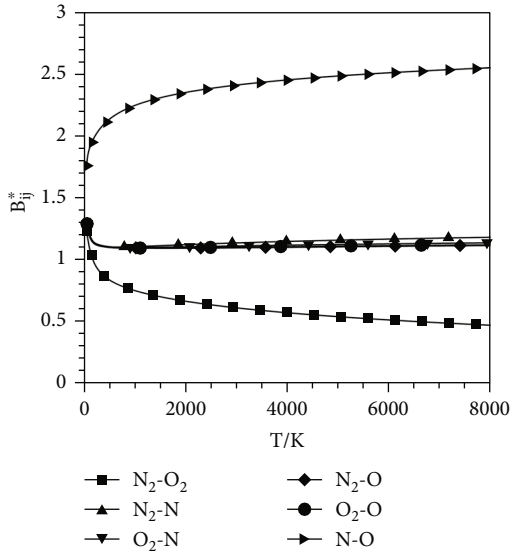

Figure 8: B_{ij}^* between neutral species.

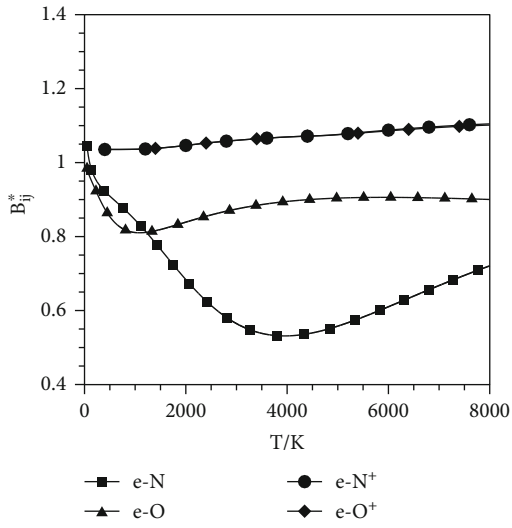

Figure 9: B_{ij}^* related to electrons.

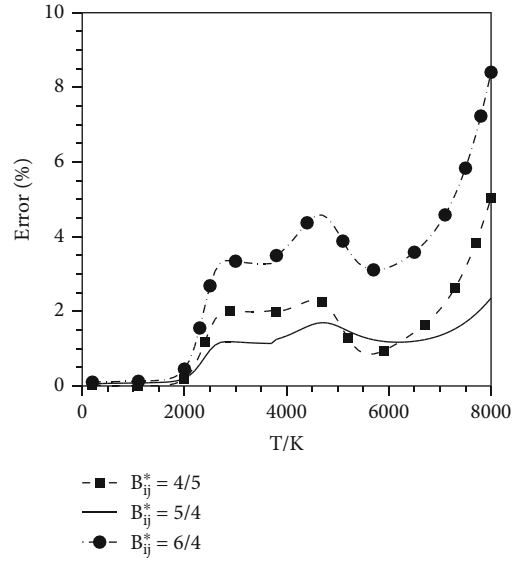

Figure 10: Relative deviation of translational thermal conductivity between equation (5) at three assumptions of B_{ij}^* and the CE method at 0.001 atm.

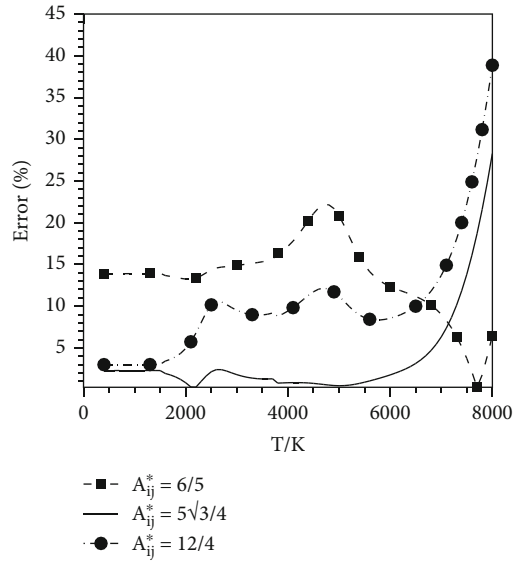

Figure 11: Relative deviation of translational thermal conductivity between equation (12) at three assumptions of A_{ij}^* and the CE method at 0.001 atm.

agreement with those of the CE method. Therefore, B_{ij}^* is taken as 5/4 for all interactions.

Different from the viscosity, the translational thermal conductivity has a different assumption for A_{ij}^*. An assumption value of A_{ij}^* larger than the actual value can compensate for the reduction of the translational thermal conductivity coefficients caused by omitting the off-diagonal elements. Figure 11 shows the relative deviation of the translational thermal conductivity between equation (12) at different assumptions of A_{ij}^* and the CE method at 0.001 atm. It can be seen that when A_{ij}^* is chosen as 6/5 (between 1.1 and 1.25), the results of equation (12) will obviously deviate from those of the CE method and so does the chosen of 12/4 for A_{ij}^*. When taking a larger value of $5\sqrt{3}/4$, the results of equation (12) are in the best agreement with those of the CE method. Therefore, simplification of $5\sqrt{3}/4$ for A_{ij}^* is selected. Besides, this value has an advantage in that the expression with a complex denominator in equation (12) can be simplified to the form of complete square:

$$k_{tr} = \sum_{i=1}^{n} \frac{\lambda_i}{1 + \sum_{\substack{j=1 \\ j \neq i}}^{n} F_{ij}^* \left(x_j / x_i\right) \left(\sqrt{6M_j}/3\right) \left(\left(\sqrt{3}M_i + M_j\right)^2 / \left(M_i + M_j\right)^{5/2}\right)}. \tag{14}$$

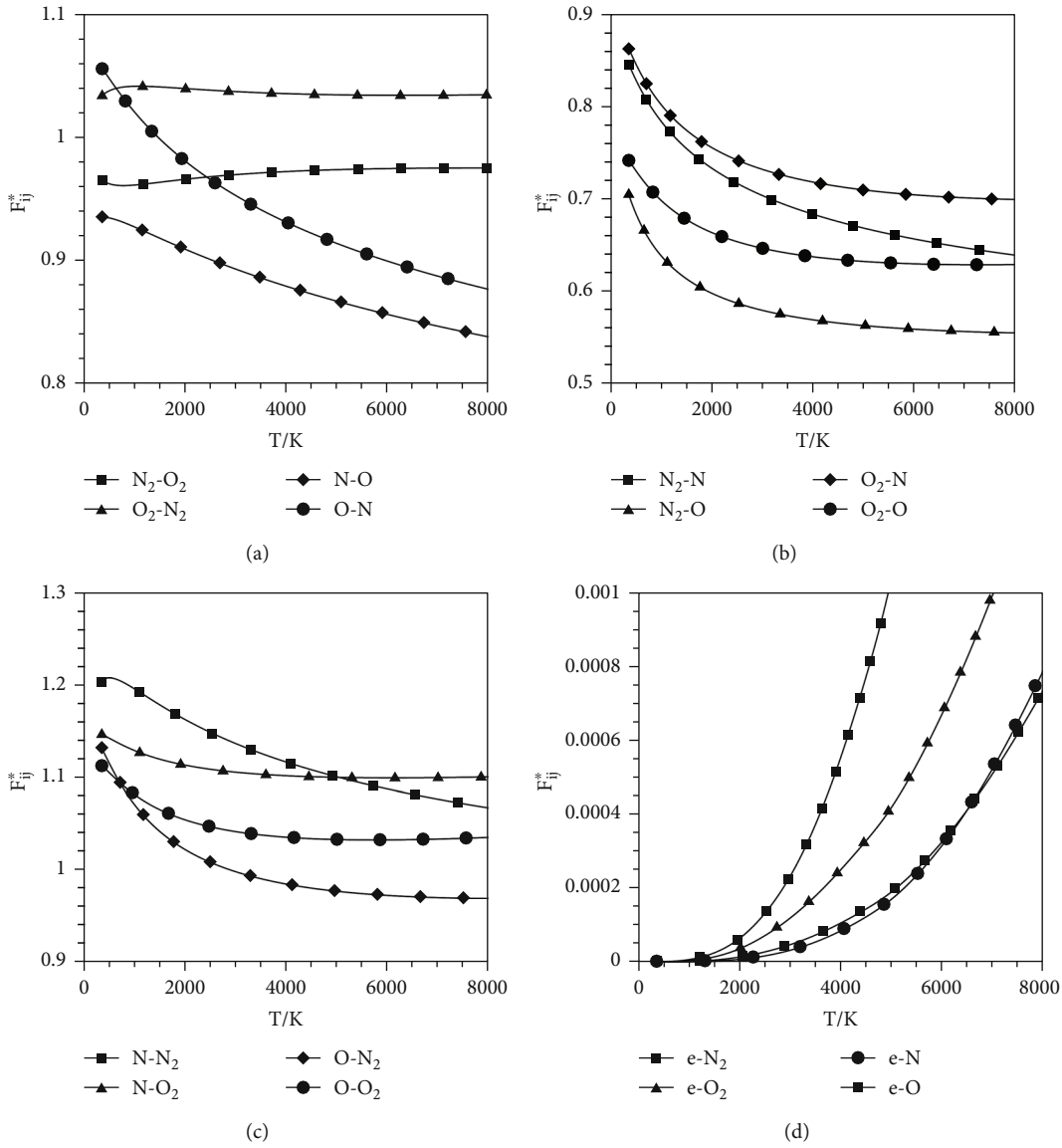

Figure 12: Reduced collision integral ratio F^*_{ij}. (a–c) F^*_{ij} related to molecules and atoms; (d) F^*_{ij} related to electrons.

Table 2: Reduced collision integral ratio F^*_{ij}.

i	j								
	N_2	O_2	N	O	NO	NO^+	e^-	N^+	O^+
N_2		1	0.67	0.57	1	1	1	1	1
O_2	1		1	1	1	1	1	1	1
N	1	1		0.88	1	1	1	1	1
O	1	1	0.88		1	1	1	1	1
NO	1	1	1	1		1	1	1	1
NO^+	1	1	1	1	1		1	1	1
e^-	0.0005	0.0005	0.0005	0.0005	1	1		1	1
N^+	1	1	1	1	1	1	1		1
O^+	1	1	1	1	1	1	1	1	

Similarly, the increment in the relative deviation curves when $T > 7000$ indicates that this assumption is applicable in the dissociation-dominated process.

3.2.4. Simplification for the Reduced Collision Integral Ratio F^*_{ij}. The final step in deriving approximate expressions (13) and (14) is to obtain an estimate of F^*_{ij}. As mentioned above, $F^*_{ij} \neq F^*_{ji}$; therefore, the simplification for F^*_{ij} and F^*_{ji} should be different. Figure 12 shows the F^*_{ij} between different species. It can be seen from Figure 12(a) that the F^*_{ij} for interactions between molecules are near 1, so the $F^*_{N_2O_2}$ and $F^*_{O_2N_2}$ can be taken as 1. The F^*_{ij} for interactions between atoms decrease monotonically from 1.05 to 0.85 with the increase of temperature. Because the collision between atoms begins to dominate at a higher temperature between 6000 K and 8000 K, the F^*_{NO} and F^*_{ON} are given a value of 0.88. Figures 12(b) and 12(c) show the F^*_{ij} for interactions

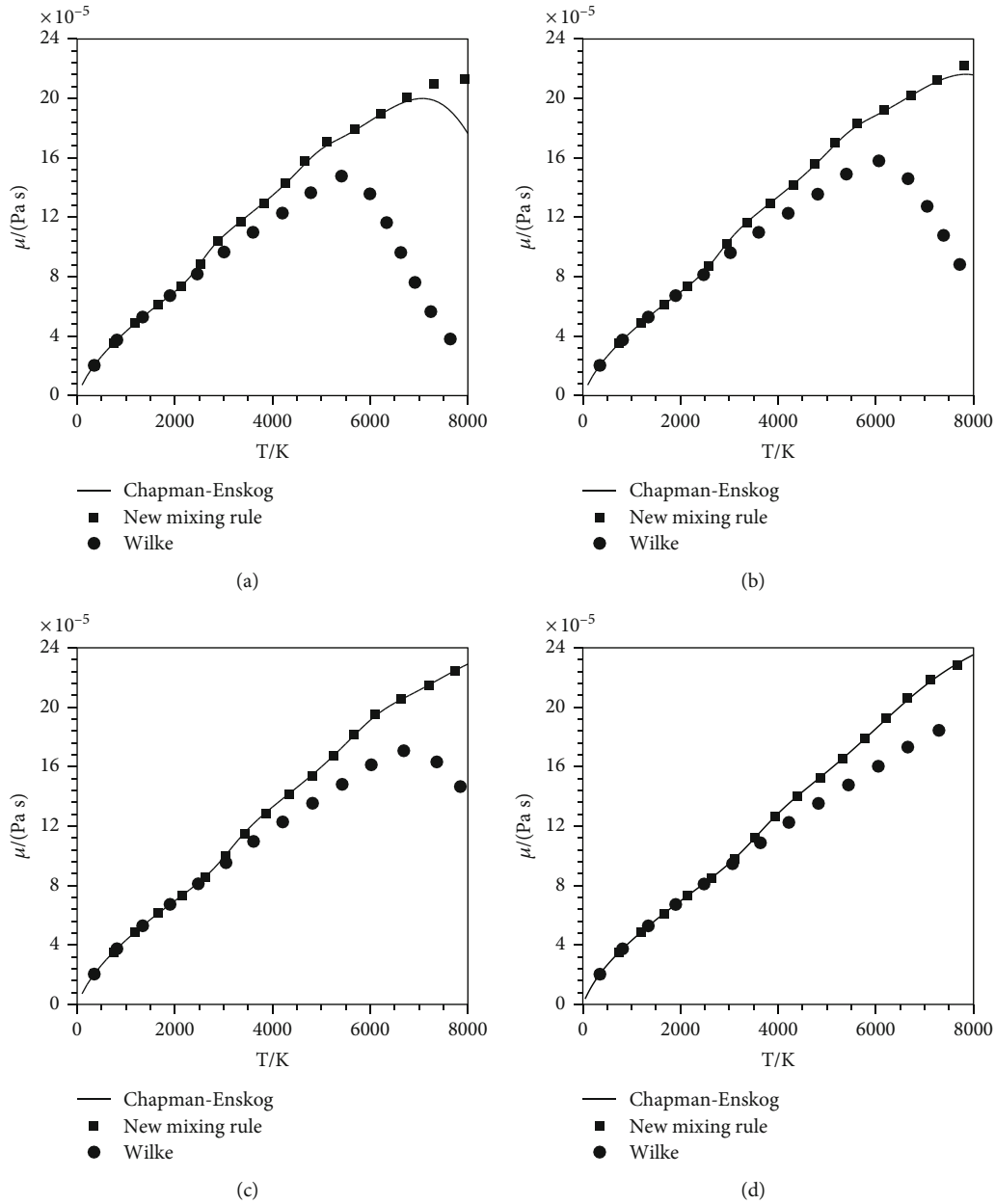

Figure 13: Viscosity coefficients by different methods. (a) 0.001 atm, (b) 0.01 atm, (c) 0.1 atm, (d) 1 atm.

between molecules and atoms. It can be seen that $F^*_{N_2N}$ decreases monotonically from 0.85 to 0.65 and $F^*_{N_2O}$ decreases monotonically from 0.7 to 0.55 with the increase of temperature, so the values of $F^*_{N_2N}$ and $F^*_{N_2O}$ can be taken as 0.67 and 0.57, respectively. According to the data in Figures 12(b) and 12(c), the rest of F^*_{ij} for interactions between molecules and atoms are given a value of 1. The F^*_{ij} between other species has little effect on the transport coefficients, so the value is assumed equal to 1. As discussed in Sections 3.1 and 3.2 (2), in expression (14), the molecule-electron and atom-electron interactions should be considered, while the effect of ions can be ignored. It can be seen from Figure 12(d) that the $F^*_{eN_2}$, $F^*_{eO_2}$, F^*_{eN}, and F^*_{eO} increase from 0 to 0.001. In this paper, the values of $F^*_{eN_2}$, $F^*_{eO_2}$, F^*_{eN}, and F^*_{eO} are taken as 0.0005, while the values of $F^*_{N_2e}$, $F^*_{O_2e}$, F^*_{Ne}, and F^*_{Oe} can be given a value of 1 because they have little impact on the translational thermal conductivity. In summary, the values for F^*_{ij} are listed in Table 2.

With assumptions for reduced collision integral ratios A^*_{ij}, B^*_{ij}, and F^*_{ij}, the improved mixing rules (equations (13) and (14)) are proposed. When x_i, μ_i, and λ_i are obtained, the viscosity and translational thermal conductivity coefficients can be calculated efficiently. Compared with the Wilke mixing rule, the new mixing rules are also a simple formula with an explicit expression, and they are apparently more simple than other mixing rules like those of Yos [14] and Copeland [24].

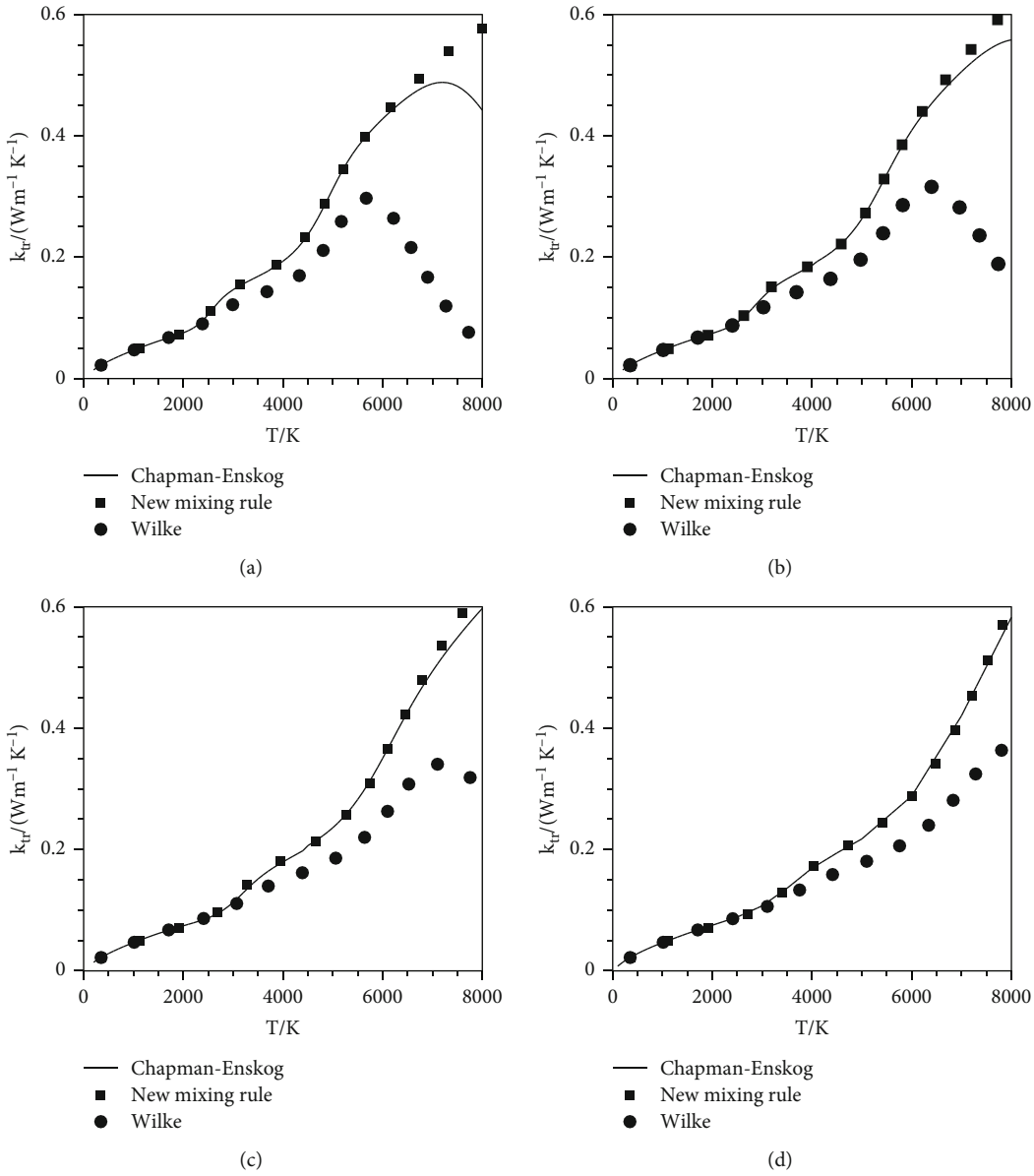

Figure 14: Translational thermal conductivity coefficients by different methods. (a) 0.001 atm, (b) 0.01 atm, (c) 0.1 atm, and (d) 1 atm.

3.3. Validation of the New Simplified Mixing Rules. The validation is conducted using the same viscosity (μ_i) and translational thermal conductivity coefficient (λ_i) expression for each species [17]. Figures 13 and 14 present a comparison of the viscosity and translational thermal conductivity using different methods (the Wilke mixing rule, the new simplified mixing rule, and the CE method) at four different pressures from 0.001 atm to 1 atm. Figure 13(a) shows a comparison of viscosity at $P = 0.001$ atm. It can be seen that the results between these methods do not differ greatly before dissociation occurs ($T < 2000$ K). However, when dissociation occurs ($T > 2000$ K), the Wilke mixing rule produces an obvious lower result than the CE method. Specifically, when $T > 5000$ K, the viscosity of the Wilke mixing rule begins to decrease, which leads to an apparent deviation. However, the new simplified mixing rule agrees excellently with the CE method, besides a small deviation when $T > 7000$ K, which is caused by ionization. Figures 13(b)–13(d) give similar results of viscosity coefficients at $P = 0.01$ atm, 0.1 atm, and 1 atm. Figures 14(a)–14(d) show a comparison of translational thermal conductivity at $P = 0.001$ atm, 0.01 atm, 0.1 atm, and 1 atm, respectively. Similar to the viscosity, the new simplified mixing rule for translational thermal conductivity has a good match with the CE method. Figure 15 shows the deviation between the mixing rules (the Wilke mixing rule and the new simplified mixing rule) and the CE method. Compared with the Wilke mixing rule, the error between the new simplified mixing rules and the CE method is significantly small. In addition, this error becomes especially smaller at great pressure. In a word, the new simplified mixing rules can accurately calculate the viscosity and translational thermal conductivity coefficients of high-

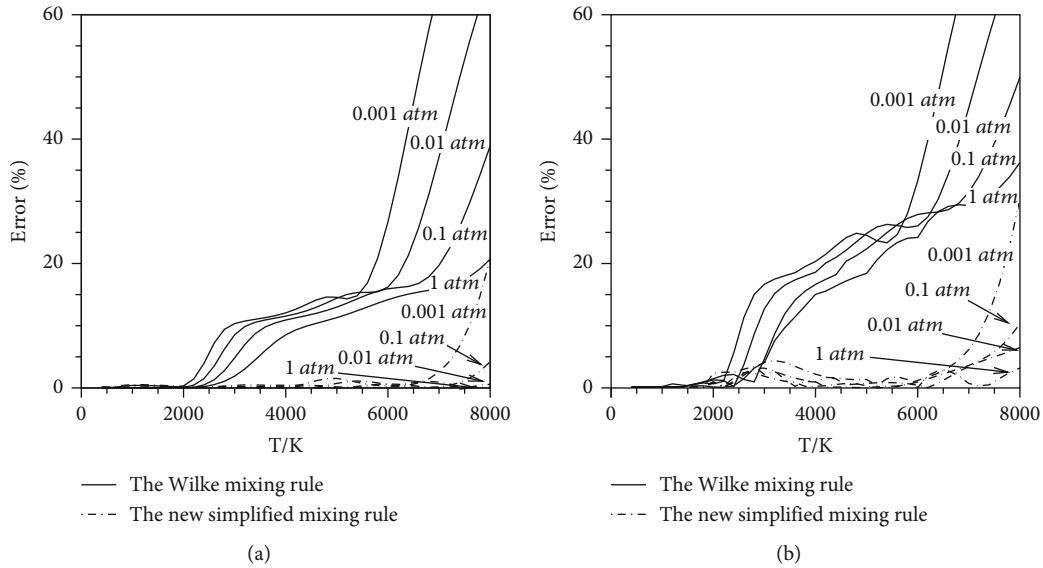

Figure 15: The deviation between the mixing rules (the Wilke mixing rule and the new simplified mixing rule) and the CE method. (a) Viscosity; (b) translational thermal conductivity.

temperature air before significant ionization occurs. The greater the pressure, the wider the temperature range applicable to the new simplified rules.

4. Conclusions

In this paper, the viscosity and translational thermal conductivity coefficients for high-temperature air are calculated. The results of the different-species model at different pressures and temperatures show that the 9-species air model is applicable for calculating the viscosity and translational thermal conductivity coefficients before significant ionization occurs. The diagonal elements' magnitude of the transport matrix indicates that collision related to the electrons has a little impact on viscosity but has a great influence on translational thermal conductivity.

To simplify the expression of the viscosity and translational thermal conductivity coefficients from a matrix equation to only an algebraic summation, the off-diagonal elements of the transport matrix are omitted. To determine the viscosity, the reduced collision integral ratio A_{ij}^* is assumed as 5/3 for all interactions. To determine the translational thermal conductivity, the reduced collision integral ratio A_{ij}^* is assumed as $5\sqrt{3}/4$, and the reduced collision integral ratio B_{ij}^* is assumed as 5/4 for all interactions. The values for F_{ij}^* are taken as different values for different species, which are summarized in Table 2. These approximations of the reduced collision integral ratio can make up contributions from off-diagonal elements which are omitted in the derivation. Based on these assumptions, the improved mixing rules (equations (13) and (14)) for viscosity and translational thermal conductivity coefficients of high-temperature air have been developed. It has a simple explicit formula, similar to the Wilke mixing rule. Rather than numerically solving the matrix equations, the new simplified mixing rules require only viscosity/translational thermal conductivity coefficients and mole fraction of each species. These rules have been extensively tested and compared with the Wilke mixing rule. The results of the new simplified mixing rules are obviously more accurate than those of the Wilke mixing rule. The new simplified mixing rules can accurately calculate the viscosity and translational thermal conductivity coefficients of high-temperature air when dissociation or weak ionization occurs.

Nomenclature

μ:	The viscosity coefficients
μ_i:	The viscosity of pure species i
x_i:	The mole fraction of species i
n:	The number of species
$\overline{b_{j0}}(1)$, $\overline{a_{j1}}(2)$:	Sonine expansion coefficients
A_{ij}^*, B_{ij}^*, F_{ij}^*:	A ratio of reduced collision integral
$\Omega_{ij}^{(l,s)*}$:	The reduced collision integrals between species i and species j
μ_{ij}:	The collision viscosity between species i and species j
λ_{ij}:	The collision translational thermal conductivity between species i and species j
k_{tr}:	The translational thermal conductivity coefficients
λ_i:	The translational thermal conductivity of species i
M_i:	The molecular weight of the species i
R:	The universal gas constant
H, **L**:	Matrix elements.

Data Availability

The data that support the findings of this study are available from the corresponding author upon reasonable request.

Conflicts of Interest

The authors have no conflicts of interest to disclose.

Authors' Contributions

Wang Zhe and Han Yufeng contributed equally to this work.

Acknowledgments

This work was supported by the National Natural Science Foundation of China (Nos. 11732011 and 12102297).

References

[1] M. R. Malik and E. C. Anderson, "Real gas effects on hypersonic boundary-layer stability," *Physics of Fluids A: Fluid Dynamics*, vol. 3, no. 5, pp. 803–821, 1991.

[2] D. X. Xiong, Y. S. Xu, and Z. Y. Guo, "Molecular dynamics simulation on thermodynamic properties and transport coefficients," *Journal of Thermal Science*, vol. 5, no. 3, pp. 196–200, 1996.

[3] T. K. Bose and T. K. Bose, "High temperature gas dynamics," in *High Temperature Gas Dynamics*, pp. 259–281, Springer, Berlin, Heidelberg, 2004.

[4] R. B. Bird, W. E. Stewart, and E. N. Lightfoot, *Transport Phenomena*, John Wiley & Sons, New York, 2nd edition, 2006.

[5] Y. Tian, G. Lin, and J. Guo, "Analysis of mass diffusion theory and models for high-temperature multi- component gases," *International Journal of Heat and Mass Transfer*, vol. 181, article 121994, 2021.

[6] J. O. Hirschfelder, C. F. Curtiss, and R. B. Bird, "Molecular theory of gases and liquids," *Physics Today 8.3*, vol. 17, p. 17, 1955.

[7] S. Chapman and T. G. Cowling, *The Mathematical Theory of Non-uniform Gases: An Account of the Kinetic Theory of Viscosity, Thermal Conduction and Diffusion in Gases*, Cambridge university press, 1990.

[8] R. S. Devoto, "Simplified expressions for the transport properties of ionized monatomic gases," *Physics of Fluids*, vol. 10, no. 10, pp. 2105–2112, 1967.

[9] C. Bonnefoi, J. Aubreton, and J. M. Mexmain, "New approach taking into account elastic and inelastic processes, for transport properties of a two temperature plasma," *Zeitschrift für Naturforschung A*, vol. 40, no. 9, pp. 885–891, 1985.

[10] G. V. Candler and R. W. MacCormack, "Computation of weakly ionized hypersonic flows in thermochemical nonequilibrium," *Journal of Thermophysics and Heat Transfer*, vol. 5, no. 3, pp. 266–273, 1991.

[11] C. P. Knisely and X. L. Zhong, "Sound radiation by supersonic unstable modes in hypersonic blunt cone boundary layers. I. Linear stability theory," *Physics of Fluids*, vol. 31, no. 2, article 024103, 2019.

[12] L. Zanus, F. Miró Miró, and F. Pinna, "Weak non-parallel effects on chemically reacting hypersonic boundary layer stability," in *AIAA Aviation 2019 Forum*, Dallas, Texas, June 2019.

[13] K. S. Yun and E. A. Mason, "Collision integrals for the transport properties of dissociating air at high temperatures," *Physics of Fluids*, vol. 5, no. 4, pp. 380–386, 1962.

[14] J. M. Yos, *Transport properties of nitrogen, hydrogen, oxygen, and air to 30,000 K*, Research & Advanced Development Division Avco Corporation Technical Memorandum, 1963.

[15] R. N. Gupta, J. M. Yos, and R. A. Thompson, *A Review of Reaction Rates and Thermodynamic and Transport Properties for the 11-Species Air Model for Chemical and Thermal Nonequilibrium Calculations to 30000 K*, Nasa Sti/recon Technical Report N, 1989.

[16] A. B. Murphy, "Transport coefficients of air, argon-air, nitrogen-air, and oxygen-air plasmas," *Plasma Chemistry and Plasma Processing*, vol. 15, no. 2, pp. 279–307, 1995.

[17] M. Capitelli, R. Celiberto, C. Gorse, and D. Giordano, "Transport properties of high temperature air components: a review," *Plasma Chemistry and Plasma Processing*, vol. 16, no. S1, pp. S267–S302, 1995.

[18] M. Capitelli, C. Gorse, S. Longo, and D. Giordano, "Collision integrals of high-temperature air species," *Journal of Thermophysics and Heat Transfer*, vol. 14, no. 2, pp. 259–268, 2000.

[19] A. D'Angola, G. Colonna, C. Gorse, and M. Capitelli, "Thermodynamic and transport properties in equilibrium air plasmas in a wide pressure and temperature range," *The European Physical Journal D*, vol. 46, no. 1, pp. 129–150, 2008.

[20] M. J. Wright, D. Bose, G. E. Palmer, and E. Levin, "Recommended collision integrals for transport property computations part 1: air species," *AIAA Journal*, vol. 43, no. 12, pp. 2558–2564, 2005.

[21] J. W. Buddenberg and C. R. Wilke, "Calculation of gas mixture viscosities," *Industrial & Engineering Chemistry*, vol. 41, no. 7, pp. 1345–1347, 1949.

[22] S. Chen and Q. H. Sun, "A quasi-one-dimensional model for hypersonic reactive flow along the stagnation streamline," *Chinese Journal of Aeronautics*, vol. 29, no. 6, pp. 1517–1526, 2016.

[23] J. A. Hao, J. Y. Wang, and C. Lee, "Numerical study of hypersonic flows over reentry configurations with different chemical nonequilibrium models," *Acta Astronautica*, vol. 126, pp. 1–10, 2016.

[24] D. Copeland, "New approximate formulas for the viscosity and thermal conductivity of gas mixtures," in *40th AIAA Aerospace Sciences Meeting & Exhibit*, Reno, NV, USA, 2002.

[25] E. A. Mason and S. C. Saxena, "Approximate formula for the thermal conductivity of gas mixtures," *Physics of Fluids*, vol. 1, no. 5, pp. 361–369, 1958.

[26] R. S. Brokaw, "Approximate formulas for the viscosity and thermal conductivity of gas mixtures. II," *The Journal of Chemical Physics*, vol. 42, no. 4, pp. 1140–1146, 1965.

[27] B. Armaly and K. Sutton, "Viscosity of multicomponent partially ionized gas mixtures," in *15th Thermophysics Conference*, Snowmass,CO,U.S.A, 1980.

[28] G. Palmer and G. Palmer, "An assessment of transport property methodologies for hypersonic flows," in *35th Aerospace Sciences Meeting and Exhibit*, Reno,NV,U.S.A, 1997 Jan.

[29] G. E. Palmer and M. J. Wright, "Comparison of methods to compute high-temperature gas viscosity," *Journal of Thermophysics and Heat Transfer*, vol. 17, no. 2, pp. 232–239, 2003.

[30] G. Palmer and M. Wright, "A comparison of methods to compute high-temperature gas thermal conductivity," in *36th AIAA Thermophysics Conference*, Orlando, Florida, 2003 June.

[31] C. F. Hansen, *Approximations for the thermodynamic and transport properties of high-temperature air*, National Advisory Committee for Aeronautics, 1958.

[32] S. Srinivasan, J. C. Tannehill, and K. J. Weilmuenster, *Simplified curve fits for the thermodynamic properties of equilibrium air, final report iowa state univ of science & technology*, no. L-16276, 1987.

[33] J. N. Butler and R. S. Brokaw, "Thermal conductivity of gas mixtures in chemical equilibrium," *The Journal of Chemical Physics*, vol. 26, no. 6, pp. 1636–1643, 1957.